

## Measurements of the Vertical Heat Flux in the Upper Ocean Layer

JACK A. C. KAISER AND KINGSLEY G. WILLIAMS

*Ocean Sciences Division, U. S. Naval Research Laboratory, Washington, D. C. 20375*

(Manuscript received 24 April 1973, in revised form 29 October 1973)

### ABSTRACT

By measuring the time rate of change of temperature in the upper 65 m of the sea at night with a precision sounding device, the amount of heat transported upward at various depths and through the sea surface as a function of time during the night was determined. The heat flux through any surface of depth  $z$  was given by  $e^{-\alpha t} (1 - Az^3)$  for  $z < z_{\max}$  (40–65 m). The amount of heat released from the sea surface ranged from 1.34 to 0.311  $\text{ly min}^{-1}$ , the release rate decreasing with time after sunset.

The data also allowed estimates of the spatially averaged thermal boundary layer thickness in the sea surface, 0.2 cm or less.

### 1. Introduction

Measurements will be described which allowed the calculation of vertical heat transfer in the upper 60 m of the ocean at night as a function of depth and time after sunset, and permitted estimates of some quantities associated with the surface thermal boundary layer. Since there is little or no nocturnal radiative heating of the water below the surface, the time rate of decrease of the temperature is directly related to the horizontal and vertical transfer of heat in the water. If the horizontal transports can be measured, or cases found when they are small enough to be neglected, then the vertical heat transfer rate can be determined (Section 2). To test this idea, measurements were made near Bermuda on six nights. On two of these nights the horizontal transports appeared, on the basis of internal evidence, to be small and determinable enough (see Section 4) to satisfy our basic assumption, thus allowing calculation of the vertical heat flux.

Great interest has been vested in the sea-air interface mainly because of the great energy source the ocean represents for the atmosphere; hence, much effort has gone into determining the energy efflux into the atmosphere. These measurements have been concentrated on the air side of the interface, and relatively little attention has been directed toward measurements in the water. Such subsurface measurements will yield similar data and will give the spatial and temporal variation of the heat transfer in the water. These measurements can be made more simply in some cases under water than in the atmosphere.

Several determinations of the vertical heat flux have been made from subsurface temperature data. Lavorko (1970) determined the upward heat flux in the upper 2 m of the Black Sea under quiet conditions. Shonting (1964) used standard BT soundings to examine the diurnal temperature variations induced in the upper

20 m of the sea and found the total amount of increase of the internal energy of the water to be about balanced by the solar insolation. Recently, Delnore (1972) published an analysis of BOMEX data, where, by using Bissett-Berman soundings from the five ships stationed in the BOMEX array, he was able to calculate a thermal energy budget for the ocean mixed layer on a diurnal scale. In particular, he found nocturnal cooling rates (measured over a 2–4 hr period) which yielded upward fluxes as large as 1.42  $\text{ly min}^{-1}$ .

### 2. Theory

The heat transfer equation for a volume of ocean water, using the continuity equation for an incompressible fluid, can be written as

$$\rho c_p \left[ \frac{\partial T}{\partial t} + \nabla_h \cdot (\mathbf{V}_h T) - \frac{\partial}{\partial z} (wT) \right] = K \left[ \nabla_h^2 + \frac{\partial^2}{\partial z^2} \right] T - \frac{\partial I}{\partial z}, \quad (1)$$

where  $\rho$  is the density,  $c_p$  the specific heat,  $\mathbf{V}_h$  the horizontal velocity vector,  $w$  the vertical velocity (positive upward),  $z$  the vertical coordinate (positive downward),  $T$  the temperature,  $K$  the thermal conductivity coefficient of sea water,  $I$  the total downwelling less upwelling irradiance, and  $\nabla_h^2$  the horizontal Laplacian. The assumption used on  $I$  is that the net sideways irradiance is zero through all vertical surfaces. Integrating once from  $z_1$  to  $z_2$  ( $z_1 < z_2$ ), we have

$$\frac{\partial}{\partial t} \int_{z_1}^{z_2} \rho c_p T dz + \int_{z_1}^{z_2} [\rho c_p \nabla_h \cdot (\mathbf{V}_h T) - K \nabla_h^2 T] dz = \left( wT + K \frac{\partial T}{\partial z} \right) \Big|_{z_1}^{z_2} - I(z_2, t) + I(z_1, t). \quad (2)$$

The second integral on the left-hand side represents the total horizontal transport of heat,  $\mathcal{H}_h(z_1, z_2, t)$ . The term on the far right is the negative of the total vertical heat transfer rate,  $H(z_1, z_2, t)$ . If we choose our lower depth  $z_2$  large enough,  $I(z_2, t) \approx 0$  and  $H(z_1, z_2, t) \approx 0$ , i.e., diurnal variations become vanishingly small below  $z_2$ . This will become evident in our data [Delnore (1972) gave values of 18 to 37 m for  $z_2$ ]. Then letting  $z = z_1$ , and  $\mathcal{H}_h(z_1, z_2, t) = \mathcal{H}_h$  and  $H(z_1, z_2, t) = H(z, t)$ , Eq. (2) becomes

$$H(z, t) = -\frac{\partial}{\partial t} \int_z^{z_2} \rho c_p T dz + I(z, t) + \mathcal{H}_h. \quad (3)$$

Now  $I(z, t)$  represents the net irradiance through the level  $z$ . If we consider the *nighttime* situation,  $I(z, t)$  approaches zero everywhere in the water except within a few micrometers of the surface, so the heat transfer rate can be conveniently determined from  $T(z, t)$  data using (3) once  $\mathcal{H}_h$  is known.

### 3. Measurement technique

The data were obtained by taking hourly temperature soundings off the starboard side of the USNS *Mizar* while she was making way at 2 kt or less. Approximately 145 soundings were taken over two 3-day periods and of these data series, two sets of data are used, 5–6 December 1972 (set I) and 9–10 December 1972 (set II). The choice of these data sets was governed by the determinancy of  $\mathcal{H}_h$  as detailed in Section 4. The posi-

tions of the ship tracks where the data were taken is shown in Fig. 1. The ship was 60–130 n mi west of Bermuda and the ocean depth always exceeded 2500 fathoms as the bottom contours show. Available XBT surface temperatures taken in the region of interest during the periods in which the measurements were made are plotted on Fig. 1. These indicate a surface thermal structure with at most slowly varying temperatures.

The sounding device consisted of a pressure sensor and a calibrated thermistor with a time constant of about 7 sec. The long time constant smoothed out small-scale fluctuations but also necessitated slow ascent and descent rates, typically  $12 \text{ m min}^{-1}$ . After the thermistor was lowered into the water, 120 sec elapsed before descent to allow the sensor to come to thermal equilibrium with the water. The nominal depth of equilibration was 1.25 m, but due to ship pitch and roll, the sensor sometimes oscillated in depth, typically between about 0.5 and 2 m during the equilibration period. At the end of each descent the thermistor was allowed to remain at maximum depth for 60 sec before starting ascent. Where the ascent temperatures differed from those of descent, the  $T(z)$  curve was obtained by taking an arithmetic mean at each level. Typically, the two temperatures differed by less than  $0.02^\circ\text{C}$ ; in extreme cases the difference was  $0.1^\circ\text{C}$ .

The pressure sensor and thermistor were each arms of two dc Wheatstone bridges whose outputs were fed into an  $x, y$  plotter giving directly a temperature-depth

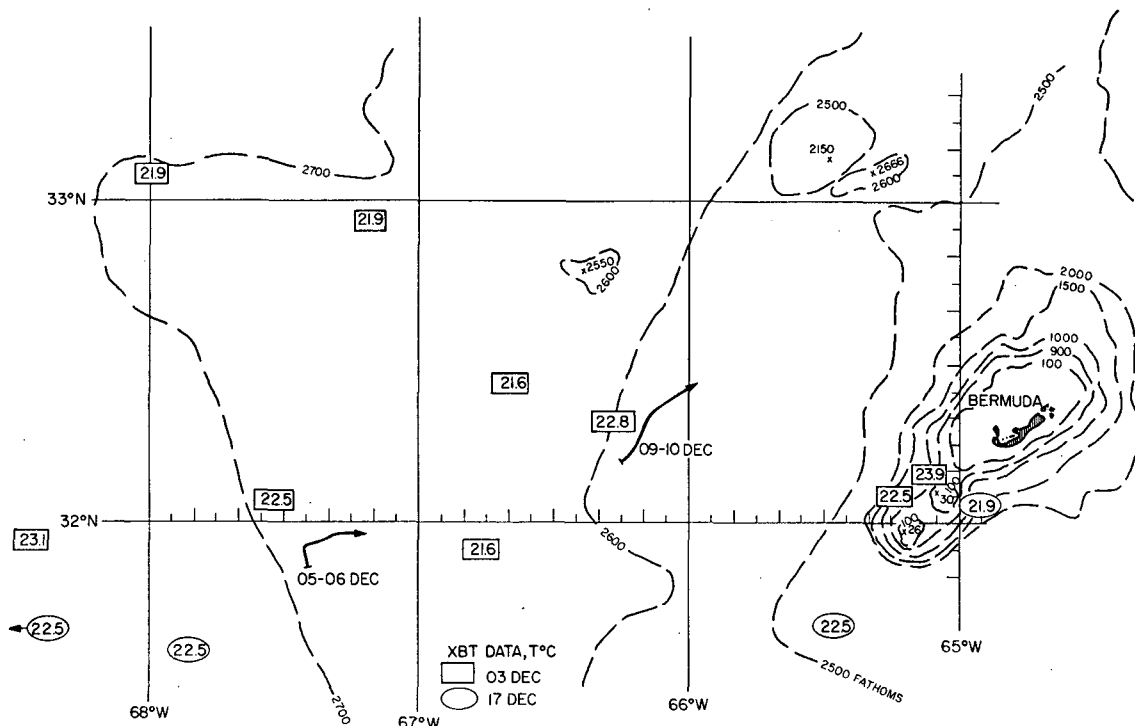


FIG. 1. Map of the data area with cruise tracks and available XBT surface temperature data.

curve. Sensitivities of the recorder were  $0.08\text{C cm}^{-1}$  and  $4\text{ m cm}^{-1}$ , allowing temperature and depth resolution to better than  $0.01\text{C}$  and  $0.5\text{ m}$ . Both the thermistor and pressure sensor were calibrated by the precision calibration group at the Naval Research Laboratory before use. While the data were being taken, the  $x,y$  plotter was periodically calibrated against  $0.1\%$  resistors. The absolute temperature error of the data is less than  $0.05\text{C}$  and the relative error (total variability of each set of data) less than  $0.02\text{C}$ .

#### 4. Sample data and meteorological conditions

During both measuring periods the synoptic situation was very similar. In period I, the sampling track was on the western edge of a high pressure area with a frontal system about  $500\text{ n mi}$  north. In period II the front was again about  $500\text{ n mi}$  north, but this time the track was in an extensive high pressure ridge extending east-west. The frontal system had been periodically pushing into the Bermuda area but never moving any great distance south of the measuring site.

For both sets of data the relative humidity at deck level ( $\sim 3\text{ m}$ ) averaged about  $80\%$ . The only significant difference between the two sets was in the wind. For set I it was from the east at  $10\text{--}31\text{ kt}$ , while during set II the wind started out at  $5\text{--}8\text{ kt}$  from the southeast at sunset on the 9th and was almost calm by the following sunrise. The only significant temporal variations in meteorological conditions during the two periods occurred for the air temperature and sky cover, and the histories of these two quantities are plotted in Fig. 2. In both cases the air temperature at deck level rose  $3\text{--}4\text{C}$  during the day while the sky was generally broken to overcast during the day. In both cases the sky became clear near sunset time. From set I the dominant sky cover was altostratus while for set II it was stratocumulus and cumulus.

In Fig. 2 is plotted the temporal history of the water temperature at four levels as determined from the sounding data. Even though there was a moderate amount of cloud cover at times, a large amount of daytime heating of the water is evident. The temperature at the  $64.5\text{ m}$  depth in set I increased about  $0.007\text{C hr}^{-1}$  but in a somewhat irregular fashion from 1400 (all times Atlantic Standard) on the 5th to 0300 on the 6th. This may be due to a small horizontal heat flow (relative to the ship) in the water. In data set II there is a slow steady decrease of  $0.005\text{C hr}^{-1}$  in the  $64.5\text{ m}$  temperature which again may be due to relative horizontal transports.

According to (3),  $\mathcal{H}_h$  needs to be known to calculate  $H[z,t]$ . In both sets of data it is assumed that  $\mathcal{H}_h$  is represented by the drift of  $T(64.5\text{ m}, t)$  so that

$$\mathcal{H}_h = \rho c_p \frac{\partial}{\partial t} \int_z^{64.5\text{ m}} T(64.5, t) dz; \quad (4)$$

thus, in (3)

$$H(z, t) = -\frac{\partial}{\partial t} \int_z^{64.5} \rho c_p [T(z', t) - T(64.5, t)] dz'. \quad (5)$$

So, in both measurement cases, (5) was used to calculate  $H(z, t)$ . In set I the "smoothed" curve was used in place of the more irregular curve to represent  $T(64.5, t)$ . The actual values of  $\mathcal{H}_h$  as determined from (4) are equivalent to surface heat fluxes of  $-0.7$  and  $+0.5\text{ ly min}^{-1}$ , respectively.

In set I there is not a continuous record of  $T(64.5)$  throughout a 24-hr period but there is in set II. The use of  $T - T(64.5)$  in place of  $T$  in the latter case is essentially the same as requiring the total heat content of the water to come back to its original value after 24 hr, based on Fig. 2. This then neglects the annual temperature trend compared to the diurnal change.

The apparent heating and cooling rates are not smoothly varying but somewhat irregular, as Fig. 2 indicates. Since the ship was making way, it was passing through small thermal inhomogeneities in the water of an estimated scale of kilometers, possibly associated with similar irregularities in the cloud cover. In principle, one would like to average over an area of a few square kilometers to remove these. This is, in effect, done by temporal smoothing, such as for the "smoothed" curve of Fig. 2, because of the headway of the ship.

Typical temperature soundings from both data sets are shown in Fig. 3. On the left are the soundings as averaged from the descent and ascent records, on the right the same soundings after they have been corrected for the temperature drift at  $64.5\text{ m}$ . For set I the cooling extends below  $60\text{ m}$ , while for set II essentially all the nocturnal cooling has occurred above  $45\text{ m}$ .

These depths agree with the depth to which solar heating was expected. Jerlov (1961) classifies the waters in the vicinity of Bermuda as optical type I to IB. For these types about  $10\text{--}25\%$  of the surface irradiance at  $0.465\text{ }\mu\text{m}$ , representing less than  $1\%$  of the solar energy, will penetrate to  $60\text{ m}$ .

#### 5. The vertical heat flux

##### a. Through the surface

The quantity

$$\delta H(z, t) = \int_0^z \rho c_p [T(z', t) - T(64.5, t)] dz' \quad (6)$$

represents the internal energy stored in a unit column of sea water between the surface and the depth  $z$ . This is determined from the soundings and plotted as a function of time in Fig. 4 for various depths. The measurements of set I were interrupted after 0230 but for set II continued through the night. The value of  $\delta H(z, t)$  decreased with time at all levels after sunset until sunrise. The heavy curve labelled  $64.5\text{ m}$  in Fig. 4 represents the

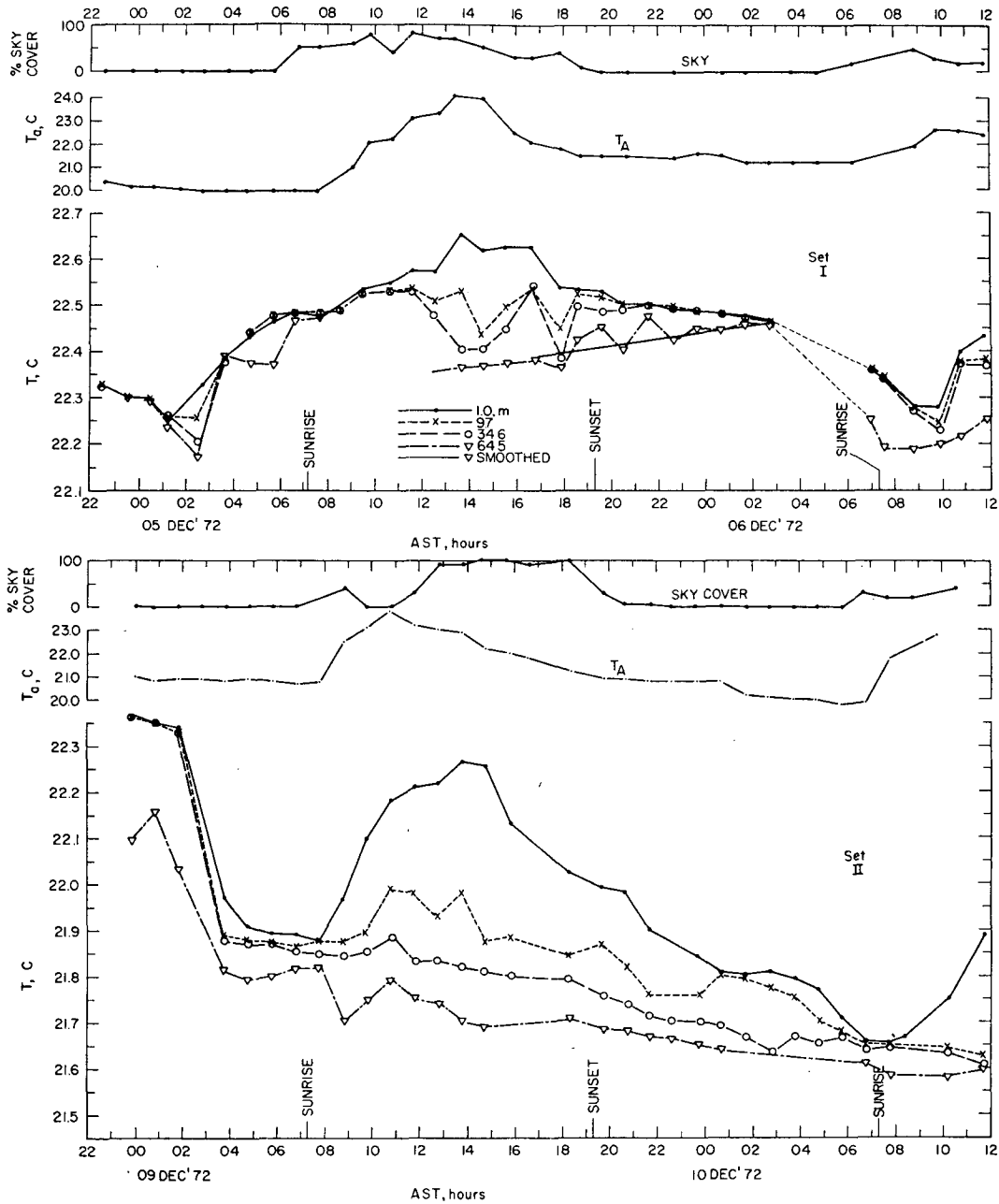


FIG. 2. Plots of the time evolution of the water temperatures at several depths, the air temperature  $T_a$ , and the amount of sky cover during the two periods of data used for this study.

total amount of heat stored in a  $1 \text{ cm}^2$  column of water,  $\delta H(64.5, t)$ . To a first approximation, it decreases exponentially in time, so a smoothed curve, justified as explained previously, to represent  $\delta H(64.5, t)$  developed by fitting a least-squares curve to the data for each 64.5 m curve, is given by

$$\delta H(64.5, t) = H_0 e^{-\alpha t}, \quad (7)$$

where  $H_0$  is the total heat excess at sunset. The observed values of  $H_0$  and  $\alpha$  are given in Table 1.

The total heat flux  $F(t)$ , through the sea surface, is then given by

$$F(t) = -\frac{\partial}{\partial t} \delta H(64.5, t) = -\alpha H_0 e^{-\alpha t}, \quad (8)$$

the negative value indicating an upward flux.

The total surface heat flux rates for several times of night are given in Table 1, as calculated from (8). The largest nocturnal rate occurs about at sunset and is

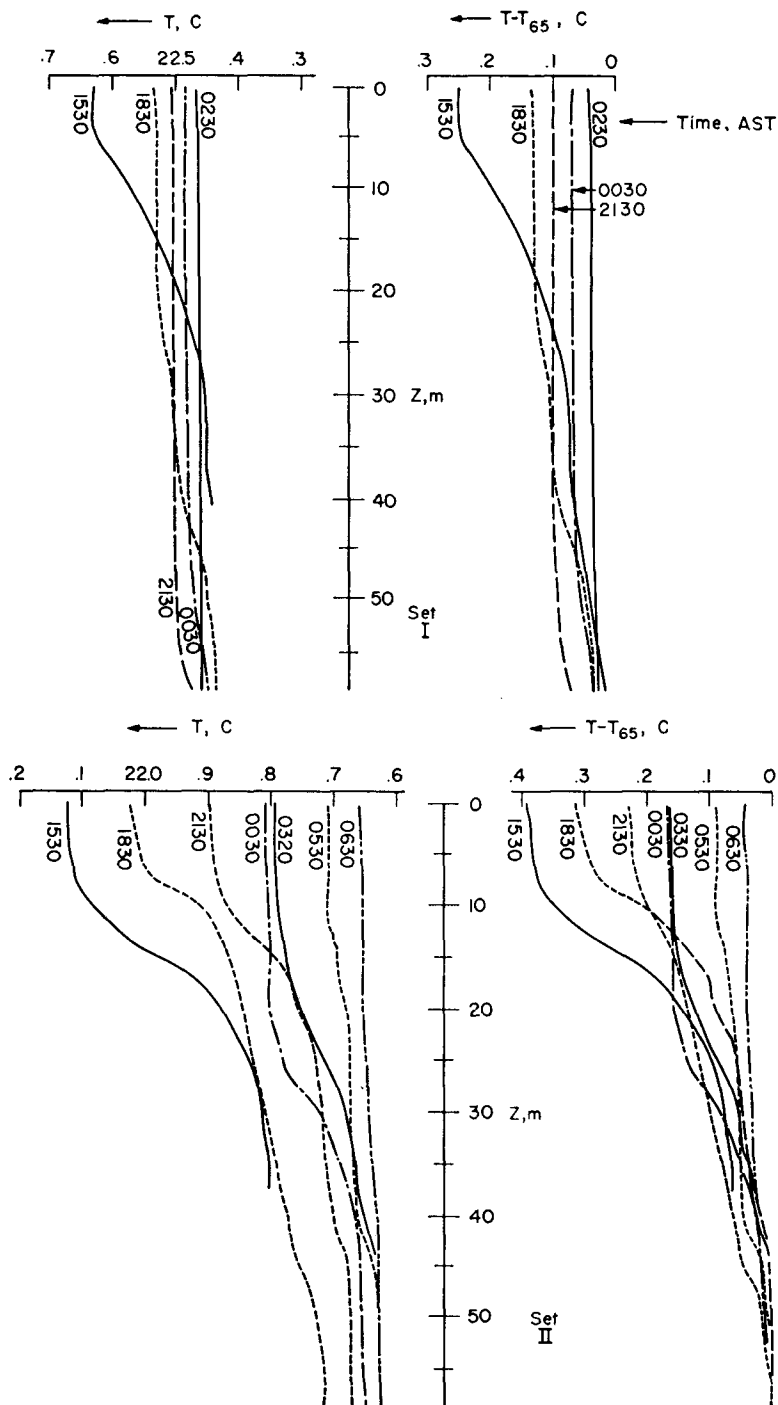


FIG. 3. Sample sounding data for the two sets of data. On the left are the actual  $T(z)$  curves while those on the right are differences from the temperature at 64.5 m.

$1.34 \text{ ly min}^{-1}$ , slightly smaller than the largest value Delnore (1972) reports. The “nocturnal average” would occur if the column of water cooled linearly with time throughout the night. Other published values for  $F(t)$  are available from measurements made over a

short period of time, e.g., an hour or so, as compared to daily or longer period averages. McAlister *et al.* (1971) find values ranging from  $0.05 \text{ ly min}^{-1}$  during intermittent rain up to  $0.45 \text{ ly min}^{-1}$  at 0500 local time on a day characterized by the authors as “best weather.”

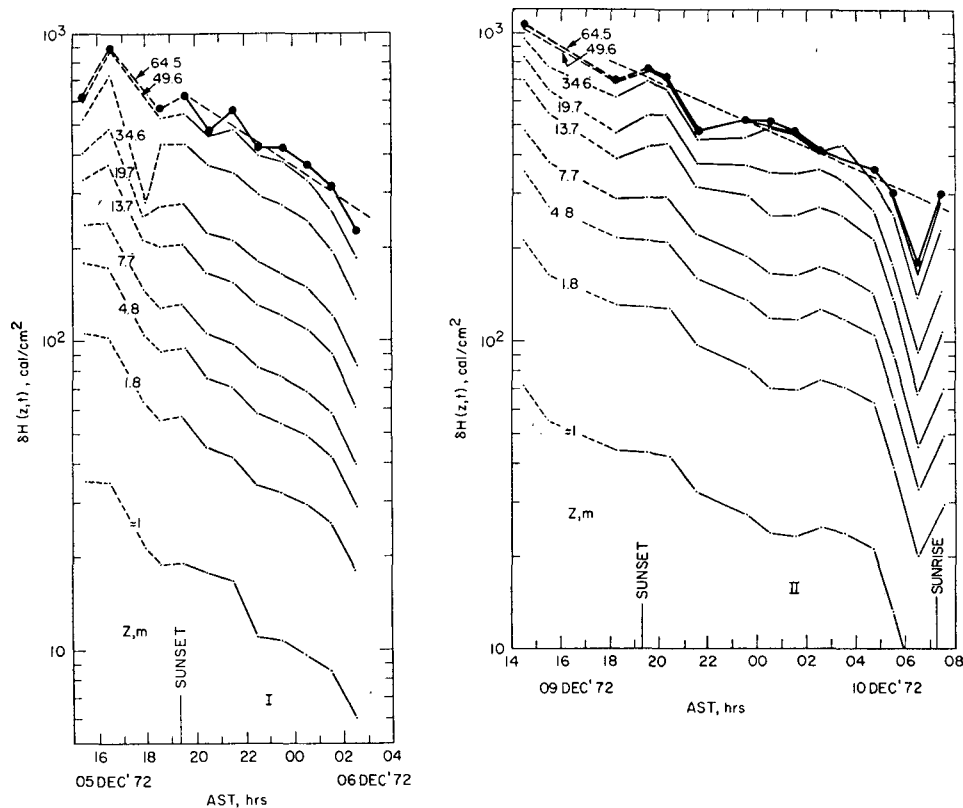


FIG. 4. The total heat content between the surface and the indicated depth as a function of time for two cases. The faint dashed line at the upper end of each plot is the least-squares fit to the 64.5 m curve after sunset.

This latter value is about equal to our early morning values. These values were obtained during the BOMEX measurements.

The *e*-folding time for heat loss from the sea,  $\alpha^{-1}$ , ranged from 8 to 11 hr.

*b. Through any level z*

It is interesting to note in Fig. 4 that the curves for each *z* are essentially parallel, suggesting that for any

two levels  $z_m$  and  $z_n$ ,  $\delta H(z_m, t) / \delta H(z_n, t)$  is approximately independent of time.

For  $z_m = z$  and  $z_n = z_2$  [ $= 64.5$  m], this ratio is plotted in Fig. 5. For set II there does appear to be a small decrease in  $\delta H(z) \delta / H(z_2)$  as time progresses. To show this, data prior to 0200 are represented by dots, and data obtained after that by crosses. The dashed line is the least-squares fit to the crosses, and the solid line the fit to the dots. In both sets of data the equation represented by the least-squares fit is

$$\delta H(z, t) / \delta H(z_2, t) = Az^b, \tag{9}$$

with the values of *A* and *b* given in Table 2. The 1.0 m data points do not lie on the straight line through the other data points, possibly due to the proximity of the ship. Also, the true depth of these data is uncertain due to ship roll and surface waves of 0.1–1 m, so they have

TABLE 1. Total heat flux quantities.

Quantity	Data set	
	I	II
$H_0$ [cal cm <sup>-2</sup> ]	645	730
$\alpha$ (sec <sup>-1</sup> )	$3.46 \times 10^{-5}$	$2.53 \times 10^{-5}$
$\alpha$ (min <sup>-1</sup> )	$2.07 \times 10^{-3}$	$1.52 \times 10^{-3}$
$\alpha^{-1}$ (hr)	8.06	11.0
$F(t)$ [ly min <sup>-1</sup> ]		
Sunset	1.34	1.11
0000 AST	0.767	0.755
0300 AST	0.528	0.593
Sunrise	0.311*	0.429
Nocturnal average	0.692*	0.629
Time when average realized	0050 AST	0215 AST

\* Based on extrapolation of Eq. (9) to sunrise.

TABLE 2. Constants of Eq. (9).

Data set	<i>A</i> (cgs units)	<i>b</i>	$z_{max}$ (m)
I	$2.49 \times 10^{-3}$	0.676	70
II, before 0200 AST	$6.11 \times 10^{-3}$	0.627	38
II, after 0200 AST	$4.84 \times 10^{-3}$	0.640	42

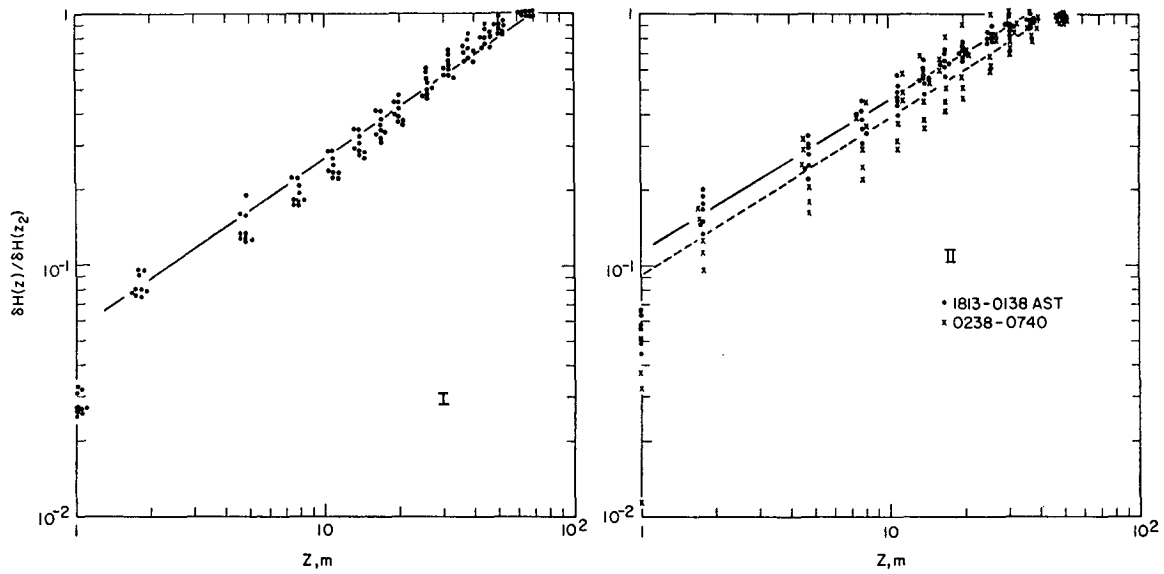


FIG. 5. The amount of heat excess in the layer above the depth  $z$  normalized with respect to the total amount of excess heat for the two sets of data. The dashed line on the right is fitted to the  $\times$ 's.

been omitted from the analysis. If their effective average depth was 0.5 m, they would then lie on the least-squares line.

From (5) and (6), the total upward heat flux through any level  $z$  is

$$H(z,t) = \frac{\partial}{\partial t} [\delta H(z,t) - \delta H(z_2,t)], \quad (10)$$

and, normalized with respect to the surface heat flux, it is

$$H'(z,t) = H(z,t)/F(t) = Az^b - 1, \quad (11)$$

which can be written

$$H'(z,t) = \left( \frac{z}{z_{\max}} \right)^b - 1, \quad (12)$$

where  $z_{\max} = A^{-1/b}$ .

The curve derived from (12) is shown in Fig. 6. In the 1.5 m thick layer near the surface 10% of the total heat loss is occurring for  $z_{\max} = 50$  m, or 90% of the upward flux is through the  $z = 1.5$  m surface. Fifty percent of the upward flux occurs through the 17.5 m surface.

The quantity  $z_{\max}$  is the depth at which  $H' = 0$  and is effectively the maximum depth to which solar heating occurred the previous day. One would expect  $z_{\max}$  to be almost solely a function of the penetration depth of solar radiation in the water and hence related directly to the water optical type (Jerlov, 1961). For our measurements,  $z_{\max}$  is given in Table 2.

### 6. The surface thermal boundary layer structure

The characteristics of a thermal boundary layer at the surface of the ocean has been of much interest recently.

Wu (1971) found thicknesses varying from 4 mm at wind velocities of about  $1 \text{ m sec}^{-1}$  to 0.04 mm at  $10 \text{ m sec}^{-1}$ , based on wind-stress coefficient measurements and the results for a heated plate at zero incidence and with small free-stream velocity. Temperature drops across this layer of 0.6C have been observed by Ewing and McAlister (1960), and values of 0.4C or so have been calculated by Saunders (1967).

From the data obtained during these measurements, one can estimate the spatially averaged vertical thermal gradient which exists at the sea surface by assuming the heat transfer process is purely conductive there.

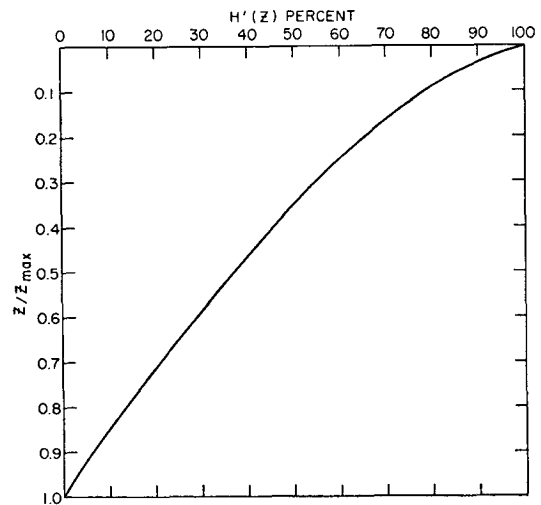


FIG. 6. The normalized total upward heat flux through the surface  $z$ .

TABLE 3. Boundary layer quantities.

Quantities	Data set	
	I	II
$F(t)$ [ $\text{ly min}^{-1}$ ]		
Average	0.692	0.629
Range*	1.34–0.31	1.11–0.43
$\partial T/\partial z$ [ $^{\circ}\text{C cm}^{-1}$ ]		
Average	8.06	7.32
Range*	15.6–3.6	13.8–5.5
$u$ [ $\text{m sec}^{-1}$ ]	6	2
$\delta$ [ $\text{cm}$ ]		
Estimated	0.15	0.20
From Wu (1971)	0.09	0.20
$\Delta T$ [ $^{\circ}\text{C}$ ]	1.2	1.5

\* Sunset to sunrise range.

These estimates range from 15.6C  $\text{cm}^{-1}$  down to 5C  $\text{cm}^{-1}$ . The values for sets I and II are given in Table 3.

A reasonable upper limit on the temperature drop across this boundary layer is the difference between the temperature of the air and that of the near-sea-surface. In our case the air temperature was measured at deck level (about 3m above the sea surface) while our near-sea-surface temperatures represent values averaged over the upper meter or so. At 1400 the air is generally at or above the sea temperature; it subsequently cools to a more or less constant value  $\Delta T$  below the near-sea-surface temperature (Fig. 2). This value of  $\Delta T$  is attained within 1 hr of sunset. For our sets of data  $\Delta T$  was 1.2C and 1.5C.

From these  $\Delta T$  values an *upper limit* on the thickness of a thermal boundary layer in the water at the sea surface can be estimated. The estimate can only be regarded as an upper limit since the air temperature increases toward the sea surface. The calculated thicknesses  $\delta$  are 0.15 and 0.30 cm, respectively.

Wu (1971) made estimates of sea-surface boundary layer thicknesses based on wind speed. For the speeds encountered during our measurements, Wu's estimate gives thicknesses of 0.09–0.20 cm, in reasonable agreement with ours. All the quantities associated with the sea-surface thermal boundary layer for sets I and II are presented in Table 3.

## 7. Conclusions

The method employed has yielded reasonable values of the total heat transfer through the sea surface as a function of the time during the night and also the heat transfer across any horizontal surface below the sea surface. The time-dependence of this heat transfer generally indicates a decrease with time after sunset. The amount of heat being transported upward through a horizontal surface at any time is  $F(t)(1-Az^3)$ . Estimates of the thermal boundary layer in the sea at the surface of about 0.2 cm agree well with other estimates.

Only two principal assumptions went into the determinations of heat flux: 1) the shorter term ( $\sim 1$  hr) temporal irregularities observed were, in fact, spatial inhomogeneities, so that temporal (and thus spatial) averages give a representative picture of the sea; 2) small temperature drifts at depth were indicative of small horizontal heat fluxes and were removed from the final values by the data-averaging procedure.

*Acknowledgments.* The authors thank the Naval Research Laboratory for providing ship time and other services necessary to accomplish these measurements. Also, the authors wish to acknowledge the XBT data supplied by Mr. Al Fisher of the Naval Oceanographic Office. One author (Jack A. C. Kaiser) held a Presidential Internship during this work.

## REFERENCES

- Defant, A., 1961: *Physical Oceanography*, Vol. 1. New York, Pergamon, 729 pp.
- Delnore, V. E., 1972: Diurnal variation of temperature and energy budget for the oceanic mixed layer during BOMEX. *J. Phys. Oceanogr.*, **2**, 239–247.
- Ewing, G., and E. D. McAlister, 1960: On the thermal boundary layer of the ocean. *Science*, **131**, 1374–1376.
- Jerlov, N. G., 1961: *Optical Oceanography*. Amsterdam, Elsevier, 194 pp.
- Lavorko, V. S., 1970: Turbulent exchange and heat flux in the water near the sea surface. *Izv. Atmos. Oceanic Phys.*, **6**, 578–579.
- McAlister, E. D., W. McLeish, and E. A. Corduan, 1971: Airborne measurements of the total heat flux from the sea during BOMEX. *J. Geophys. Res.*, **76**, 4172–4180.
- Saunders, P. M., 1967: The temperature at the ocean-air interface. *J. Atmos. Sci.*, **24**, 269–273.
- Shonting, D. H., 1964: Observations of short-term heating of the layers of the ocean. Report U. S. Naval Underwater Ordinance Station, Newport, R. I., 22 pp.
- Wu, J., 1971: An estimation of oceanic thermal-sublayer thickness. *J. Phys. Oceanogr.*, **1**, 284–286.